Atmos. Chem. Phys. Discuss., 12, 33323–33358, 2012
www.atmos-chem-phys-discuss.net/12/33323/2012/
doi:10.5194/acpd-12-33323-2012
© Author(s) 2012. CC Attribution 3.0 License.

Atmospheric Chemistry and Physics Discussions

This discussion paper is/has been under review for the journal Atmospheric Chemistry and Physics (ACP). Please refer to the corresponding final paper in ACP if available.

Production of methyl vinyl ketone and methacrolein via the hydroperoxyl pathway of isoprene oxidation

Y. J. Liu[1], I. Herdlinger-Blatt[1,2], K. A. McKinney[3], and S. T. Martin[1,4]

[1]School of Engineering and Applied Sciences, Harvard University, Cambridge, Massachusetts, USA
[2]Institute of Ion Physics and Applied Physics, University of Innsbruck, Innsbruck, Austria
[3]Department of Chemistry, Amherst College, Amherst, Massachusetts, USA
[4]Department of Earth and Planetary Sciences, Harvard University, Cambridge, Massachusetts, USA

Received: 1 December 2012 – Accepted: 4 December 2012 – Published: 21 December 2012

Correspondence to: K. A. McKinney (kamckinney@amherst.edu),
S. T. Martin (scot_martin@harvard.edu)

Published by Copernicus Publications on behalf of the European Geosciences Union.

Abstract

The photo-oxidation chemistry of isoprene (C_5H_8) was studied in a continuous-flow chamber under conditions such that the reactions of isoprene-derived peroxyl radicals (RO_2) were dominated by hydroperoxyl (HO_2) pathway. A proton-transfer-reaction time-of-flight mass spectrometer (PTR-TOF-MS) with switchable H_3O^+ and NO^+ reagent ions was used for product analysis. The products methyl vinyl ketone (MVK; C_4H_6O) and methacrolein (MACR; C_4H_6O) were differentiated using NO^+ reagent ions. The MVK and MACR yields were 4.3 ± 0.4 % and 3.2 ± 0.3 %, respectively, for HO_2-dominant conditions at +25 °C and < 2 % relative humidity. The respective yields were 41.1 ± 2.2 % and 28.8 ± 1.2 % for NO-dominant conditions. The yields for HO_2-dominant conditions imply a concomitant yield (i.e., recycling factor) of hydrogen oxide radicals (HO_x) of 15 ± 0.7 % from the reaction of isoprene-derived RO_2 with HO_2. Other isoprene oxidation products, believed to be organic hydroperoxides, also contributed to the ion intensity at the same mass-to-charge (m/z) ratios as the MVK and MACR product ions, and these products were selectively removed from the gas phase using a variable temperature cold trap (−40 °C) in front of the PTR-TOF-MS. These hydroperoxide products were absent for NO-dominant conditions. When incorporated into regional and global chemical transport models, the yields of MVK and MACR and concomitant HO_x yields reported in this study will improve the accuracy of simulations of the HO_2 reaction pathway of isoprene, which has been shown to make a significant contribution to the total reactivity of isoprene-derived RO_2 radicals on a global scale.

1 Introduction

By abundance, isoprene (C_5H_8) is the dominant non-methane biogenic volatile organic compound (VOC) in the atmosphere, and its reactive chemistry plays an important role in the oxidative cycles of the atmosphere (Poisson et al., 2000). Isoprene oxidation is initiated for the most part by the addition of a hydroxyl radical (OH) across a double

bond followed by rapid reaction of the alkyl radical with molecular oxygen (O_2), resulting in the production of a series of isomeric hydroxyl-substituted alkyl peroxyl radicals (ISOPOO; HOC_5H_8OO) (Fig. 1). The subsequent chemistry of the ISOPOO radicals proceeds along several competing pathways: (i) reactions with nitric oxide (NO) (e.g., Tuazon and Atkinson, 1990), (ii) reactions with hydroperoxyl radicals (HO_2) (e.g., Paulot et al., 2009), (iii) self- and cross- reactions with other organic peroxyl radicals (RO_2) (Jenkin et al., 1998), and (iv) possible unimolecular isomerization reactions (Peeters et al., 2009; da Silva et al., 2010; Crounse et al., 2011). As illustrated in Fig. 2, under real atmospheric conditions, the NO and HO_2 pathways are the major competing reaction pathways determining the fate of ISOPOO (Crounse et al., 2011). The RO_2 pathway is less important because of low atmospheric VOC concentrations (typically 10 ppt to 10 ppb level). The reaction with NO dominates in polluted, urban regions of the planet (Fig. 2). Many isoprene source regions, particularly remote tropical forests, however, are characterized by sufficiently low NO_x concentrations (e.g., Lelieveld et al., 2008) that the HO_2 pathway dominates. The HO_2 pathway is estimated to account globally for 53.5 % of the reactive fate of ISOPOO radicals (Crounse et al., 2011).

There remain significant uncertainties in the branching ratios and principal products of isoprene photo-oxidation for the HO_2 reaction pathway. Mechanisms employed in many regional and global models, including the near-explicit Master Chemical Mechanism (MCM v3.2) (Jenkin et al., 1997; Saunders et al., 2003), treat the reaction of HO_2 with ISOPOO as a radical-termination reaction, as follows (R1a):

$$\mathrm{ISOPOO + HO_2 \rightarrow ISOPOOH + O_2} \quad \text{(R1a)}$$

in which organic hydroperoxides (ISOPOOH; HOC_5H_8OOH) are formed with 100 % yield. A competing, less investigated pathway, however, might also be important (Dillon and Crowley, 2008) (R1b):

$$\mathrm{ISOPOO + HO_2 \rightarrow ISOPO + OH + O_2} \quad \text{(R1b)}$$

This pathway produces alkoxy radicals (ISOPO, HOC_5H_8O) and recycles the OH radicals (recalling that the oxidation pathway was initiated by OH attack on isoprene).

Although the same type of reaction has been demonstrated in the laboratory only for carbonyl-bearing RO_2 radicals (i.e., not HOC_5H_8OO) (Hasson et al., 2004; Jenkin et al., 2007, 2008; Dillon and Crowley, 2008), theoretical studies suggest that it may occur for peroxyl radicals in the form of RCHXOO and $RCHXCH_2OO$ in general, where X is an electronegative atom, through a hydrotetroxide intermediate (Hasson et al., 2005). The internal hydrogen bonding between the hyrotetroxide and X lowers the energy of the intermediate and transition state (Hasson et al., 2005). As shown in Fig. 1, two major ISOPOO radicals, ISOPBOO and ISOPDOO, are in the above form, but the other two, ISOPAOO and ISOPCOO, are not. Hence Reaction (R1b) may not occur for ISOPAOO and ISOPCOO.

Methyl vinyl ketone (MVK, C_4H_6O) and methacrolein (MACR, C_4H_6O) arise from the decomposition of the two alkoxy isomers produced by reaction (R1b) (cf. Fig. 1):

$$\mathrm{ISOPBO \xrightarrow{O_2} MVK + HCHO + HO_2} \quad \text{(R2)}$$

$$\mathrm{ISOPDO \xrightarrow{O_2} MACR + HCHO + HO_2} \quad \text{(R3)}$$

Radical termination by Reaction (R1a) does not produce MVK or MACR. Hence, the yields of MVK and MACR can serve as tracers for the occurrence of Reaction (R1b). The experimental strategy of the present study is to take advantage of the different yields of MVK and MACR following (R1a) and (R1b) to assess the importance of the latter in the reaction of isoprene with OH under HO_2-dominant conditions.

The isoprene photo-oxidation experiments described herein were conducted in a continuous-flow chamber. Efforts were made to ensure and to verify that the HO_2 pathway was the dominant fate of the ISOPOO species, as opposed to NO pathway or RO_2 cross reactions. The yields of MVK and MACR were separately determined using a proton-transfer-reaction time-of-flight mass spectrometer (PTR-TOF-MS) with switchable reagent ion capability (H_3O^+, NO^+).

2 Experimental

The reaction conditions for seven different isoprene photo-oxidation experiments are listed in Table 1. Experiments #1 to #6 correspond to HO_2-dominant conditions and Experiment #7 to NO-dominant conditions. For Experiments #1 to #6, the reaction of H_2O_2 with OH radicals was used to produce HO_2 radicals: $OH + H_2O_2 \rightarrow HO_2 + H_2O$. For Experiment #7, a flow of NO into the chamber in the absence of H_2O_2 was used, so that the HO_2 pathway was not important under these conditions. Experiment #1 was the main experiment. For Experiments #2 through #6, the value of one chamber parameters was halved or doubled relative to Experiment #1 as an approach to validate experimentally (i) that MVK and MACR were first-generation products and (ii) that the HO_2 pathway was dominant (cf. Sect. 3.2–3.3). Experiment #7 for NO-dominant conditions facilitated comparison of our results to those reported previously in the literature for the yields of MVK and MACR under high-NO_x conditions.

2.1 Harvard Environmental Chamber (HEC)

The experiments were carried out in the Harvard Environmental Chamber (Fig. S1). Detailed descriptions of the chamber were published previously (Shilling et al., 2009; King et al., 2010). The chamber was operated as a continuously mixed flow reactor (CMFR), with balanced inflows and outflows. A new polyfluoroalkoxy (PFA) Teflon bag with a volume of 5.3 m^3 was installed for these experiments. The mean reactor residence time was varied from 1.8 to 7.4 h. Temperature and relative humidity were held at 25 ± 1 °C and < 2 %, respectively.

For the HO_2-dominant Experiments (#1 to #6), isoprene (50 ppm in nitrogen, Scott Specialty Gases), hydrogen peroxide (31.50 wt %, *Trace*SELECT® Ultra, Fluka), and dry air (pure air generator, Aadco 737) were continuously injected. Isoprene concentrations were 59 to 118 ppb in the inflow and 10 to 35 ppb in the outflow from the chamber bag depending on reaction conditions (Table 1). A commercially-available ultra pure H_2O_2 solution was used to minimize the content of nitrogen impurity as confirmed by

NO and NO_x measurements. Compared to earlier experiments using the HEC (King et al., 2010), an updated H_2O_2 injection system was used to improve stability. An H_2O_2 solution was continuously introduced by a syringe pump into a warmed glass bulb. The syringe pump was housed in a refrigerator at 4 °C to avoid H_2O_2 decomposition. Dry air at a flow rate of 1–4 sLpm was blown through the bulb to evaporate the injected H_2O_2 solution and carry it into the chamber bag. Within the CMFR, photolysis of H_2O_2 by ultraviolet light produced OH radicals, initiating isoprene oxidation. For the NO-dominant Experiment (#7), NO (1.02 ppm NO in nitrogen with 0.01 ppm NO_2 impurity; Scott Specialty Gases) was injected in place of H_2O_2 to produce an inflow concentration of 28.2 ppb NO and 0.03 ppb NO_2. Coupled NO_x and HO_x photochemical cycles were initiated by photolysis of NO_2. The injected NO contributed to increasing the OH concentration by promoting the conversion of HO_2 to OH: $HO_2 + NO \rightarrow OH + NO_2$.

The outflow from the HEC was sampled by a PTR-TOF-MS, a condensation particle counter (CPC, TSI 3022A), an ozone monitor (Teledyne 400E), and a high-sensitivity NO_x analyzer (Eco Physics CLD 899 Y). The CPC instrument was used to measure the background number concentration of particles in the HEC, which was below 0.5 cm^{-3} during the experiments. This low particle number concentration suggests insignificant new particle production. The NO concentration was below the detection limit (3σ) of 70 ppt for Experiments #1 to #6. The ozone monitor was used to estimate the H_2O_2 concentration in Experiments #1 to #6 by using the ratio of the absorption cross-section of H_2O_2 to that of O_3 (254 nm) under the assumption that absorption was dominated by H_2O_2. The H_2O_2 concentration measured by this method was 6.7 to 26 ppm for Experiments #1 to #6. The expected concentration based on in-flow concentrations but not accounting for physical and reactive losses inside the chamber bag was 8.0 to 32 ppm.

2.2 Mass spectrometry

A proton-transfer-reaction time-of-flight mass spectrometry (PTR-TOF-MS 8000, Ionicon Analytik GmbH, Austria) equipped with switchable reagent ion capacity was used to

measure the concentrations of gaseous organic species in the chamber. For sampling, chamber air was pulled through a PFA sample line at a total flow rate of 1.25 sLpm. The PTR-TOF-MS sub-sampled from this flow at a rate of 0.25 sLpm, resulting in a transit time of 4 s between the chamber and the instrument.

The PTR-TOF-MS was described by Jordan et al. (2009a,b) and Graus et al. (2010). In the present study, either H_3O^+ or NO^+ reagent ions were generated in the ion source and used to selectively ionize organic molecules in the sample air. The use of NO^+ reagent ions allows separation of isomeric aldehydes and ketones (Blake et al., 2006), specifically MVK and MACR. The chemical ionization reaction by NO^+ or H_3O^+ is soft, typically resulting in little fragmentation, although relatively weakly bound species can still undergo some fragmentation in the drift tube (Smith and Spanel, 2005). The high-resolution TOF detector (Tofwerk AG, Switzerland) was used to analyze the reagent and product ions and allowed for exact identification of the ion molecular formula (mass resolution > 4000).

A calibration system was used to establish the instrument sensitivities to isoprene, MVK, and MACR. Gas standards (5.12 ppm isoprene, 5.26 ppm MVK in N_2; 5.27 ppm MACR in N_2, Scott Specialty Gases) were added into the sample flow at controlled flow rates. In each experiment, the inlet flow was switched to dry air from the pure air generator to establish background intensities.

Settings of the drift tube were optimized to measure MVK and MACR at high sensitivity. The instrument was operated with a drift tube temperature of 60 °C and a drift tube pressure of 2.2 mbar. In H_3O^+ mode, the drift tube voltage was set to 520 V, resulting in an E/N = 118 Td (E, electric field strength; N, number density of air in the drift tube; unit, Townsend, Td; 1 Td = 10^{-17} V cm^2). In NO^+ mode, a drift tube voltage of 300 V was used, resulting in E/N = 68 Td. At this reduced E/N ratio, ionization of MVK and MACR led to distinct product ions while retaining a highly sensitive instrument response.

PTR-TOF-MS spectra were collected at a time resolution of 1 min. A custom data processing package was developed in *Mathematica* (ver 8.0, Wolfram Research, USA) to analyze the recorded mass spectra. Using this package, the relative mass deviation was less than 10 ppm over the spectrum. The package consisted of several subroutines: peak shape fitting, mass calibration, peak assignment, and signal analysis (cf. Supplement). Compared with the analysis method reported in Muller et al. (2010), the main difference was in fitting of the asymmetric peak shape. Muller et al. (2010) approximated the peak shape using the superposition of four Gaussian peaks, but this method did not work well for our peaks, possibly because of different instrument tuning. Instead, we used several well established single-ion peaks (e.g., the peak for $H_3^{18}O^+$ ion for H_3O^+ mode) to produce an empirically derived reference peak shape, which was then used in the peak fitting routine.

2.3 Low-temperature trap

The reactions of ISOPOO with HO_2 can produce C5 products that have multiple functional groups, including organic hydroperoxides ISOPOOH and its further oxidation products dihydroxyl epoxides (IEPOX; cf. Fig. S2) (Paulot et al., 2009). These products possibly fragment after collision with H_3O^+ or NO^+ in the PTR-TOF-MS (Smith and Spanel, 2005), and the resultant fragment ions may have the same m/z values as the product ions of MVK and MACR because they all inherit the carbon skeleton from isoprene. As an approach to separate possible ISOPOOH and IEPOX products from MVK and MACR, prior to injection into the PTR-TOF-MS, the outflow from the HEC was passed through a 1-m PFA coil (3/16 inch inner diameter) that was immersed in a low temperature liquid bath. As the temperature of the bath was decreased in discrete steps from +25 to −40 °C, molecules of progressively lower vapor pressures sequentially condensed in the coil and were thereby removed from the gas flow. This approach is particularly suited to separating low-volatility compounds such as ISOPOOH and IEPOX from high-volatility species like MVK and MACR. The quantification of MVK and MACR was based on PTR-TOF-MS measurements downstream of the trap at −40 °C (cf. Sect. 3.1 and Sect. 3.6 for further discussion).

2.4 Modeling with MCM v3.2

The contribution by different reaction pathways was estimated for each experiment using a kinetic box model (Chen et al., 2011). The kinetic scheme for isoprene chemistry was extracted from the MCM v3.2 via website: http://mcm.leeds.ac.uk/MCM (Jenkin et al., 1997; Saunders et al., 2003). Model runs were initialized using the conditions of each experiment (Table 1), with the exception of the H_2O_2 concentration. Instead of using the H_2O_2 injection rates as shown in Table 1, the spectroscopically measured steady-state H_2O_2 concentrations of each experiment were used as a constraint in the model. The one-sun photolysis rates of the MCM model were scaled by 0.3 to match the lower light intensity of the HEC.

3 Results and discussion

3.1 Quantification of isoprene, MVK, and MACR

The NO^+ mass spectra recorded for zero air, isoprene, MVK, and MACR standards are shown in Fig. 3. The dominant product ion of the reaction of isoprene (C_5H_8) with NO^+ was the charge-transfer ion $C_5H_8^+$ (*m*/*z* 68.0621), which is in agreement with Karl et al. (2012). NO^+ reacted with the aldehyde MACR (C_4H_6O) to yield mainly the dehydride ion $C_4H_5O^+$ (*m*/*z* 69.0335) and a small amount of the $C_4H_6O{\cdot}NO^+$ cluster ion (*m*/*z* 100.0393). NO^+ reacted with the ketone MVK (C_4H_6O) to produce mainly the $C_4H_6O{\cdot}NO^+$ cluster ion. Ion-molecule clustering reactions are favorable when no other exothermic channel is available, as is especially the case for the reaction of NO^+ with ketones (Španěl et al., 1997). The hydride ion (H^-) transfer reaction is favorable for aldehydes because extraction of the H^- ion from a -CHO moiety requires less energy than from a hydrocarbon chain. These ionization patterns have been observed for ketones and aldehydes using NO^+ in selective-ion flow-tube studies (SIFT; E/N = 0 Td)

(Španěl et al., 2002). In comparison, the proton transfer reaction of MVK and MACR with H_3O^+ gave rise dominantly to $C_4H_7O^+$ (*m*/*z* 71.0492).

The sensitivities of the PTR-TOF-MS to isoprene, MVK, and MACR are listed in Table 2 for trap temperatures of +25 and −40 °C. To account for possible matrix effects, calibrations for both $H_3O^+$and NO^+ were carried out for each experiment by standard addition to the outflow air from the chamber (i.e., prior to the low-temperature trap). For both the $H_3O^+$and NO^+ modes, the sensitivities did not depend on trap temperature. This temperature independence indicates that isoprene, MVK, and MACR did not condense at a trap temperature of −40 °C. Hence, MVK and MACR were effectively separated from other oxidation products of lower volatility by use of the trap at −40 °C (cf. Sect. 3.6). The isoprene, MVK, and MACR concentrations reported herein were based on NO^+ ionization and using the −40 °C trap prior to PTR-TOF-MS.

In an iterative process, the E/N value for NO^+ mode was optimized to isolate the product ions of MACR from those of MVK while retaining high instrument sensitivity (cf. Fig. S3). Compared with an earlier drift tube study using NO^+ (Blake et al., 2006), much less fragmentation was observed in the present study, both for MVK and MACR, possibly because of the lower drift tube energies used here (i.e., E/N = 68 Td compared to E/N = 165 Td). The good separation achieved with NO^+ enabled separate quantification of MVK and MACR in the mixed composition present in the chamber outflow. The small contribution of MACR to the $C_4H_6O{\cdot}NO^+$ cluster ion was corrected for algebraically (cf. Eqs. (S1)–(S3) in the Supplement).

As a comparison point, the sensitivity of isoprene in NO^+ mode measured in this study agreed with the value reported by Karl et al. (2012) under similar E/N ratios (cf. Supplement). With respect to calibration in H_3O^+ mode, the sensitivities of isoprene, MVK, and MACR in H_3O^+ mode differed from the theoretically expected values by less than 10 % (Zhao and Zhang, 2004; de Gouw and Warneke, 2007). The signal for $C_3H_5^+$ (*m*/*z* 41.039), which is a common fragment of isoprene in H_3O^+ mode, was 6 % of the main isoprene signal and lay within the range of 3 % to 16 % reported in the literature (e.g., Ammann et al., 2004; McKinney et al., 2011).

Table 1 presents the steady-state concentrations of isoprene, MVK, and MACR measured in NO^+ mode as well as the steady-state concentrations of isoprene and MVK + MACR measured in H_3O^+ mode determined from the data at −40 °C. The total concentration of MVK + MACR measured using H_3O^+ ionization agreed with the sum of the speciated measurements using NO^+ ionization for all Experiments #1 through #7 (R^2 = 0.9999).

3.2 MVK and MACR yields

The yield of MVK (MACR) from isoprene oxidation is equal to the sum of the mathematical products of (i) the branching ratio leading to the precursors ISOPBOO (ISOPDOO) in the initial reaction of isoprene with OH and (ii) the branching ratios to the channels forming ISOPBO (ISOPDO) in the subsequent ISOPBOO (ISOPDOO) reactions (cf. Fig. 1). Analysis of reactant and product concentrations in the CMFR at steady state provides a method for determination of the product yields. At steady state, the relationship of mass balance for the sources and sinks of MVK is as follows:

$$0 = \left(Y_{\mathrm{MVK}}\, k_1\, c\,[\mathrm{OH}]_{\mathrm{ss}}\, c\left[\mathrm{C_5H_8}\right]_{\mathrm{ss}}\right)_{\mathrm{sources}} - \left(k_2\, c\,[\mathrm{OH}]_{\mathrm{ss}}\, c\,[\mathrm{MVK}]_{\mathrm{ss}} + \frac{1}{\tau} c[\mathrm{MVK}]_{\mathrm{ss}} + k_{\mathrm{wall}}\, c[\mathrm{MVK}]_{\mathrm{ss}}\right)_{\mathrm{sinks}} \quad (1)$$

in which $c[\mathrm{M}]_{\mathrm{ss}}$ is the steady-state chamber concentration of compound M, Y_{MVK} is the yield of MVK from isoprene oxidation, τ is the mean residence time in the chamber, k_1 and k_2 are the reaction rate coefficients of isoprene and MVK with OH, respectively, and k_{wall} is the steady-state wall loss rate of MVK. Rearrangement of Eq. (1) leads to the expression for the yield of MVK, as follows:

$$Y_{\mathrm{MVK}} = \frac{\left(k_2\, c[\mathrm{OH}]_{\mathrm{ss}} + 1/\tau + k_{\mathrm{wall}}\right) c[\mathrm{MVK}]_{\mathrm{ss}}}{k_1\, c[\mathrm{OH}]_{\mathrm{ss}}\, c\left[\mathrm{C_5H_8}\right]_{\mathrm{ss}}} \quad (2)$$

For Y_{MACR}, a direct analogy to Eq. (2) exists.

For use of Eq. (2), values of k_1 and k_2 were taken from the IUPAC database (Atkinson et al., 2006). A value of $k_{\mathrm{wall}} = 0\,\mathrm{s}^{-1}$ was used based on the results of wall-loss experiments for isoprene, MVK, and MACR that were performed separately in the HEC (cf. Supplement). The value of $c[\mathrm{OH}]_{\mathrm{ss}}$ was calculated based on measurements of the isoprene concentration prior to the reaction and at steady state, as follows:

$$0 = \left(\frac{1}{\tau} c\left[\mathrm{C_5H_8}\right]_{\mathrm{in}}\right)_{\mathrm{sources}} - \left(k_1\, c[\mathrm{OH}]_{\mathrm{ss}}\, c\left[\mathrm{C_5H_8}\right]_{\mathrm{ss}} + \frac{1}{\tau} c\left[\mathrm{C_5H_8}\right]_{\mathrm{ss}}\right)_{\mathrm{sinks}} \quad (3)$$

in which $c[\mathrm{C_5H_8}]_{\mathrm{in}}$was the inflow concentration of isoprene to the HEC. The steady-state OH concentration inferred by use of Eq. (3) varied from 1.8 to $2.0 \times 10^6\,\mathrm{cm}^{-3}$ for Experiments #1 to #6.

Yields of MVK and MACR for each experiment are listed in Table 1. In the case of Experiment #1 for HO_2-dominant conditions, the MVK and MACR yields were 4.6 ± 0.3 % and 3.2 ± 0.2 %, respectively, for reaction at 25 °C and < 2 % RH. By comparison, without low-temperature trap correction, the respective yields were 22.8 ± 1.0 % and 12.6 ± 0.5 %, respectively. Based on averaging the yield data of all the valid HO_2-dominant experiments, including Experiments #1, #2, #5 and #6 (cf. Table 1 and Sect. 3.3), a MVK yield of 4.3 ± 0.4 % and a MACR yield of 3.2 ± 0.3 % are obtained.

In the case of Experiment #7 for NO-dominant conditions, MVK and MACR were produced in high yields as a result of the reaction of ISOPOO with NO (e.g., Tuazon and Atkinson, 1990). O_3 produced as part of the NO_x photochemical cycle also reacted to a small extent with isoprene, MVK, and MACR. Equations (1)–(3) were therefore expanded to include this chemistry, with rate constants taken from the IUPAC database (cf. Eqs. (S4)–(S6) in the Supplement). The ozone concentration (65 ppb) measured in the chamber outflow was used, resulting in a calculated OH concentration of $1.5 \times 10^6\,\mathrm{cm}^{-3}$ with ozone correction. For the above ozone and OH concentrations, 90 % of isoprene reacted with OH and 10 % with ozone. The ozonolysis of isoprene also provided an additional source term for MVK and MACR. This term, with MVK and MACR yields taken from Grosjean et al. (1993), was also included in the cal-

culation (cf. Eqs. (S4)–(S6) in the Supplement). The resulting MVK and MACR yields (Table 1) were 36.7 ± 1.6 % and 31.7 ± 1.0 % without ozone correction and 41.1 ± 2.2 % and 28.8 ± 1.2 % with the correction.

As a caveat for consideration, the source term in Eq. (1) is written assuming that MVK is not produced through any process other than as a first-generation product of OH reaction with isoprene. Secondary oxidation processes of some isoprene oxidation products of the HO_2 pathway, like ISOPOOH ($C_5H_{10}O_3$) and IEPOX ($C_5H_{10}O_3$), could conceivably also produce some MVK and MACR and therefore represent an additional source term. As one test of the data against this possibility, experiments were conducted for halved (#2; 1.9 h) and doubled (#3; 7.4 h) chamber residence times (relative to 3.7 h in Experiment #1). For an increase (decrease) in chamber residence time, the steady-state concentration of isoprene decreased (increased) while those of its oxidation products increased (decreased). In these experiments, the MVK and MACR yields can be expected to remain constant only in the absence of significant secondary oxidation processes, which would introduce non-linearity to the measured yields. As shown in Fig. 4a, halving the residence time (Experiment #2, Table 1) left the yield unchanged compared to Experiment #1. By comparison, doubling the residence time (Experiment #3, Table 1) increased the MVK and MACR yields. Therefore, secondary processes seemed to produce significant quantities of MVK and MACR only for $\tau \gg 3.7$ h, and shorter residence times such as in Experiment #1 produced yields representative of first-generation production.

3.3 HO_2-dominant conditions

For the conducted experiments, the dominant regime for the fate of the ISOPOO radicals, whether by reaction with HO_2, NO, or RO_2 or by isomerization, was assessed both computationally with the assistance of MCM simulations and experimentally by empirical observation of the effects of varying the reaction conditions on the results. The HO_2 and $\sum RO_2$ concentrations modeled using the MCM together with measured NO were used to calculate the contribution of each pathway to the fate of ISOPOO in

each experiment. The results are presented in Table 3. For Experiment #1, the modeled concentrations of HO_2 and $\sum RO_2$ were 540 ppt and 17 ppt, respectively, and the measured NO was below the detection limit (70 ppt), resulting in a calculated contribution of 93 % from the HO_2 pathway. This value represents a lower limit because as a stringency test the calculation used a maximum value for the NO concentration (70 ppt). Actual NO concentrations were lower because of scavenging by HO_2, perhaps on order of 3 ppt based on the model simulation. The calculated contributions of the RO_2 and isomerization pathways were negligible for all experiments.

The accuracy of the foregoing modeling analysis is subject to uncertainties in the kinetic scheme of MCM v3.2 and the reaction rate coefficients of ISOPOO via each pathway. Therefore, Experiments #4 to #6 were designed to provide further empirical verification that there was no considerable contribution to Experiment #1 from pathways other than HO_2. Experiments #4 and #5 employed halved and doubled H_2O_2 inflow concentrations, respectively, thereby changing the steady-state concentration of HO_2 (cf. Table 3). In the case that other pathways significantly competed with HO_2 (i.e., implying HO_2 was not fully dominant), the MVK and MACR yields would have increased (decreased) with a decrease (increase) of the H_2O_2 and hence HO_2 concentrations (since, as represented in MCM (v3.2), the yields of MVK and MACR are 41.5 % and 26.5 % via the NO pathway and 35.5 % and 24.5 % via the RO_2 pathway, whereas yields measured in the Experiment #1 were much lower, 4.6 ± 0.3 % and 3.2 ± 0.2 %, respectively). As shown in Fig. 4b, doubling the H_2O_2 concentration (Experiment #5, Table 1) did not decrease the yield compared with Experiment #1. Halving of the H_2O_2 concentration, however, increased the MVK and MACR yields (Experiment #4, Table 1), implying that pathways other than HO_2 made contributions to Experiment #4. The conclusion is that the NO and RO_2 pathways were not significant in Experiment #1 because of the high HO_2 concentrations.

Experiment #6 was designed as a further empirical test of the importance of the RO_2 pathway relative to the HO_2 pathway. Doubling isoprene inflow concentration in Experiment #6 increased the steady-state concentration of RO_2 (cf. Table 3) yet the

MVK and MACR yields did not increase (Fig. 4c), supporting the conclusion that the RO_2 pathway was insignificant and the HO_2 pathway dominated in Experiment #1.

3.4 Comparison with literature

Laboratory studies investigating isoprene oxidation chemistry generally have been categorized as either "high-NO_x" or "low-NO_x" experiments (Tuazon and Atkinson, 1990; Paulson et al., 1992; Miyoshi et al., 1994; Ruppert and Becker, 2000; Benkelberg et al., 2000; Sprengnether et al., 2002; Lee et al., 2005; Karl et al., 2006; Paulot et al., 2009; Navarro et al., 2011; Crounse et al., 2011). Figure 5 shows a comparison of the yields of MACR and MVK quantified in this study to the yields reported in earlier "high-NO_x" and "low-NO_x" experimental studies and also the yields represented in MCM. The yields of MVK and MACR via the NO pathway quantified in our NO-dominant experiments are in good agreement with earlier "high-NO_x" experiments. Our observations also agree with the yields used in the MCM for the NO pathway.

The yields of MVK and MACR via the HO_2 pathway reported herein are 60–90 % lower than the yields reported in other "low-NO_x" experiments (Miyoshi et al., 1994; Ruppert and Becker, 2000; Benkelberg et al., 2000; Lee et al., 2005; Navarro et al., 2011). Several factors may contribute to this difference. For all of these studies, the RO_2 pathway was expected to have a significant or even dominant contribution to the ISOPOO chemistry because high initial isoprene concentrations (1–100 ppm) were used, as illustrated in Fig. 2. Miyoshi et al. (1994) found that the yields of MVK and MACR increased for higher isoprene:H_2O_2 ratios, an experimental parameter which regulated the ratio of RO_2 to HO_2. Navarro et al. (2011) likewise reported that the yields of MVK and MACR dropped as the modeled ratio of HO_2 to RO_2 increased from 0.1 to 1. These findings suggest that both the RO_2 and the HO_2 channels contributed to the observed MVK and MACR production in these "low-NO_x" experiments, with higher yields of MVK and MACR from the RO_2 pathway than from the HO_2 pathway, as supported by currently accepted mechanisms including the MCM (Fig. 5). Another issue for some of the "low-NO_x" studies is that the background NO concentration was typi-

cally not well measured, e.g., < 100 ppb of NO_x reported in the study by Ruppert and Becker (2000). NO_x and HONO off-gassing have been observed in many chamber systems (Carter et al., 2005; Rohrer et al., 2005). In the present study we found that injection of H_2O_2 can increase the measured NO_x level in the reactor depending on the content of nitrogen impurity in the H_2O_2 solution. An unaccounted contribution from the background NO in the earlier "low-NO_x" experiments, therefore, could be another reason for the higher reported yields. The present study achieved low NO concentrations (verified experimentally to be below the detection limit of 70 ppt) by use of a high-purity H_2O_2 solution and a bag never exposed to high concentrations of NO_x and operated in a CMFR configuration.

Paulot et al. (2009) probed the HO_2 pathway using ppb-level isoprene concentrations and negative chemical ionization mass spectrometry (CIMS). A total yield of MVK and MACR was reported because the CIMS instrument did not separately measure isomeric MVK and MACR. This yield was 12 ± 12 % via the HO_2 pathway, and the large uncertainty was tied to a small initial amount of NO_x present initially in the chamber (Paulot et al., 2009). Our results (7.5 ± 0.5 % for MVK+MACR) fall into the yield range suggested by their study.

3.5 HO_x regeneration via the reaction of HO_2 and ISOPOO

The production of MVK and MACR from ISOPOO through the HO_2 reaction pathway is concomitant with OH production, according to Reaction (R1b). Therefore, the MVK and MACR yields for HO_2-dominant conditions imply a concomitant yield of hydroxyl radical from (R1b) of 7.5 ± 0.5 %. This value is slightly higher than the OH product yield reported by Dillon and Crowley (2008) (< 6 %) for another C5 radical ($HOC_5H_{10}OO$), but is consistent with more recent work from the same group, which constrained the OH yield from Reaction (R1b) to < 15 % for ISOPOO (Taraborrelli et al., 2012). Reactions (R2) and (R3), which follow Reaction (R1b), also regenerate HO_2 radicals, corresponding to a total HO_x ($OH + HO_2$) recycling ratio of 15 ± 0.7 % compared with the radical termination channel Reaction (R1a).

3.6 Organic hydroperoxides and epoxides

Changes in the signal intensities of $C_5H_8^+$, $C_4H_5O^+$, and $C_4H_6NO_2^+$ ions produced using the NO^+ reagent ion are shown in Fig. 6 for stepwise decreases in trap temperature from +25 to −40 °C. Results are shown for Experiments #1 and #7, representing HO_2-dominant and NO-dominant conditions, respectively. The ion intensities plotted in Fig. 6 nominally represent isoprene, MACR, and MVK: the data show that in the HO_2-dominant experiments additional species contributed to these ions for trap temperatures warmer than −30 °C. The more general formula $C_4H_6NO_2^+$ is therefore used in place of $C_4H_6O{\cdot}NO^+$ because specific formulas of the additional species are not known.

The signal intensity for the $C_5H_8^+$ ion did not depend on trap temperature for either dominant oxidation pathway. The implication is that there was no chemical interference for isoprene detection via the $C_5H_8^+$ ion. Likewise, the signal intensities of the $C_4H_5O^+$ and $C_4H_6NO_2^+$ ions did not depend on temperature for the NO-dominant experiments, implying that these ions represented the instrument response to MACR and MVK in those experiments. By comparison, the signal intensities of the nominal $C_4H_5O^+$ and $C_4H_6NO_2^+$ ions depended strongly on temperature from 0 to −30 °C in the HO_2-dominant experiments, implying the presence of other molecular products that were removed at low temperature. The signal intensities were independent of temperature from −30 to −40 °C, meaning that the $C_4H_5O^+$ and $C_4H_6NO_2^+$ ions at −40 °C represented the instrument response to MACR and MVK. Temperature-dependent patterns of signal intensity using the H_3O^+ reagent ions (Fig. S4) were similar to the results shown in Fig. 6 for the NO^+ reagent ions.

For the HO_2-dominant experiments, the signal intensities of the $C_4H_5O^+$ and $C_4H_6NO_2^+$ ions were stable at temperatures warmer than 0 °C. As the trap temperature cooled below 0 °C, the signal intensities first decreased and then returned to the original level. This dip-restore behavior suggests adsorption on the cold inner walls of the trap coil followed by thermodynamic equilibration between partial and vapor pres-

sures with time. As the trap temperature decreased further, the dip in signal intensity increased and the rate of signal recovery decreased, consistent with a longer approach to equilibrium for decreased vapor pressures at lower temperatures. For −30 °C, signal recovery was no longer observed, suggesting that the surface uptake process transitioned from adsorption to condensation.

With high plausibility, the condensing species can be inferred to be a mixure of organic hydroperoxides (ISOPOOH) and possibly epoxides (IEPOX) based on their physical properties and the dominant chemical pathways. There are two lines of evidence. (1) The condensing species were absent for the NO-dominant experiments, implying that the condensing products were produced exclusively by the HO_2 pathway. ISOPOOH ($C_5H_{10}O_3$) and IEPOX ($C_5H_{10}O_3$) are oxidation products formed exclusively by the HO_2 pathway. Paulot et al. (2009) reported a yield of > 70 % for ISOPOOH from the reaction of HO_2 + ISOPOO and a yield of > 75 % for IEPOX from further oxidation of ISOPOOH by OH. (2) The condensing species had lower volatilities than MVK and MACR because neither MVK nor MACR condensed at −40 °C (Table 2). Compared with MVK and MACR, the ISOPOOH and IEPOX species have multiple functional groups as well as an additional carbon atom. Correspondingly, their vapor pressures are expected to be lower than MVK and MACR (Pankow and Asher, 2008).

The expected product ions of ISOPOOH and IEPOX assuming no fragmentation were not observed in the chamber air using either H_3O^+ or NO^+ reagent ions. Therefore, either thermal decomposition in the instrument (60 °C) or fragmentation following ionization occurred to these two compounds in both modes. A set of experiments was carried out to investigate how operating parameters of the PTR-TOF-MS can influence the fragmentation or decomposition of the species condensing in the low temperature trap. The results are included in the Supplement. The conclusion of the analysis is that ionization processes rather than thermal decomposition likely explain the production of ions at m/z values identical to those of MVK and MACR.

To further assess whether ISOPOOH and IEPOX can fragment to ions at the same m/z ratio as the product ions of MVK and MACR, the fragmentation patterns for their

authentic standards or proxy compounds were tested. β-IEPOX (cf. Fig. S2), which is the most abundant IEPOX isomer produced from isoprene (Paulot et al., 2009), was synthesized following the procedure of Zhang et al. (2012). The ionization of β-IEPOX mainly led to $C_5H_7O^+$ ions in H_3O^+ mode and $C_5H_6O^+$ ions in NO^+ mode, which are different from the product ions of MVK and MACR. Under the assumption of similar fragmentation patterns for all the isomers of IEPOX, the conclusion is that IEPOX is not the condensing species that contributes to the same m/z ratio as the MVK and MACR ions.

Because no ISOPOOH standards were available, tert-butyl hydroperoxide (M = $C_4H_{10}O_3$) was instead tested as a proxy compound. The main product ions included $(M-(OOH))^+$, $(MH-(OH)-(CH_3))^+$, and $(MH-(H_2O))^+$ in H_3O^+ mode. For NO^+ mode, $(M-(OOH))^+$ and $(M\cdot NO-(OH)-(CH_3))^+$ were observed. As illustrated in Reaction (R4), the production of $(M\cdot NO-(OH)-(CH_3))^+$ in NO^+ mode can result in a loss of a β-carbon and an -OH from the -OOH group to produce a carbonyl compound upon reaction with NO^+. A similar pathway can produce $(MH-(OH)-(CH_3))^+$ in H_3O^+ mode. Under the supposition that similar chemical processes can occur for M = ISOPOOH, the product ions are identical to those produced by MVK and MACR in the PTR-TOF-MS analysis (Reactions (R5) and (R6)). A further line of evidence in favor of hydroperoxides is the variation of signal intensities with chamber residence time (cf. Fig. S5). The equivalent concentrations of the interference for MVK and MACR (defined as the difference in the concentrations of MVK and MACR quantified at the trap temperature of 25 °C and those at −40 °C) were higher for shorter residence times, suggesting that the contributing compounds are first-generation products, i.e., hydroperoxides.

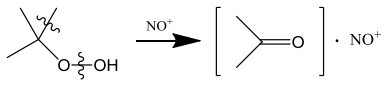

(R4)

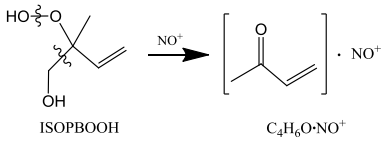

(R5)

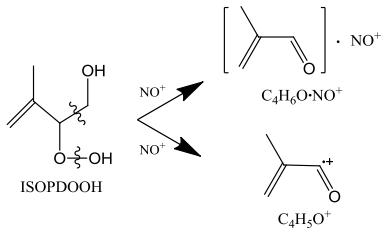

(R6)

4 Conclusions and atmospheric implications

Photo-oxidation experiments of isoprene were conducted in a steady-state chamber for HO_2-dominant and NO-dominant conditions. The concentrations of isoprene, MVK, and MACR in the chamber were measured with a PTR-TOF-MS equipped with switchable H_3O^+ and NO^+ reagent ion capacities. The use of NO^+ allowed separate quantification of isomeric MVK and MACR, which was not possible by the more commonly used H_3O^+. For both the H_3O^+ and NO^+ modes, some low-volatility oxidation products produced under HO_2-dominant conditions, possibly isoprene hydroperoxides, fragmented to ions having the same m/z ratios as the product ions of MVK and MACR. These

low-volatility compounds, which served as an interference of MVK and MACR quantification, were removed by adding a low-temperature trap (−40 °C) in the sampling line prior to the PTR-TOF-MS.

These results have implications with respect to the use of PTR-MS instruments to elucidate isoprene chemistry in clean atmospheric environments, which are typically characterized by high HO_2/NO ratios (i.e., favoring HO_2 dominant pathway) (Fig. 2). The $C_4H_7O^+$ ions in H_3O^+ mode are usually exclusively attributed to MVK and MACR (de Gouw and Warneke, 2007; Blake et al., 2009). The results of the present study, however, showed that some low-volatility oxidation products of isoprene produced via the HO_2 pathway, possibly hydroperoxides, fragment to ions at the same *m*/*z* ratios as the product ions of MVK and MACR. Caution is therefore needed with respect to interference compounds when using the PTR-MS for measurements of MVK and MACR in environments of high HO_2/NO ratios.

With respect to the yields of MVK and MACR, a steady-state approach was used in this study's analysis. This approach was validated by the good agreement between the yields measured under high-NO_x conditions and those reported in the literature. For the low-NO_x conditions of the present study, both kinetic modeling and inferential experimental evidence were consistent with HO_2 pathway as the dominant fate of ISOPOO. Under these conditions, the measured yields of MVK and MACR were 4.3 ± 0.4 % and 3.2 ± 0.3 %, respectively.

The yields of MVK and MACR reported in this study for the reaction of ISOPOO and HO_2 correspond to a concomitant HO_x yield (i.e., recycling) of 15 ± 0.7 % (Reactions (R1b), (R2) and (R3)). This HO_x recycling is not taken into account in widely employed chemical mechanisms of the atmospheric chemistry of isoprene. A growing body of observational evidence suggests significant discrepancies in modeled and measured OH concentrations in atmospheric environments having high isoprene emissions and low NO_x concentrations (e.g., Lelieveld et al., 2008; Stone et al., 2011). An OH-recycling channel for the reaction of ISOPOO and HO_2 was proposed to explain the discrepancy. Recycling of 200–300 % OH radicals (i.e., amplification) was needed

to close the gap between model predictions and atmospheric measurements over the coastal Amazon rainforest (Lelieveld et al., 2008; Butler et al., 2008) as well as in a Southeast Asian rainforest (Stone et al., 2011). Therefore, the present study's result of 15 ± 0.7 % for HO_x recycling is insufficient to close the gap. Other OH-recycling mechanisms may therefore be important (Peeters et al., 2009; Crounse et al., 2011). Another possibility, suggested by a recent report on instrumental issues, could be that the gap between measured and modeled OH was not so large as originally reported (Mao et al., 2012).

Supplementary material related to this article is available online at: http://www.atmos-chem-phys-discuss.net/12/33323/2012/acpd-12-33323-2012-supplement.pdf.

Acknowledgements. This material is based upon work supported by the National Science Foundation under Grant No. ATM-0959452. Y. J. Liu acknowledges support from the NASA Earth and Space Science fellowship program. We acknowledge the Thomson lab from Northwestern University for synthesis of β-epoxide and Mikinori Kuwata, Ben Langford, Franz Geiger, Fabien Paulot and Alfons Jordan for useful discussion and assistance with the experiments.

References

Ammann, C., Spirig, C., Neftel, A., Steinbacher, M., Komenda, M., and Schaub, A.: Application of PTR-MS for measurements of biogenic VOC in a deciduous forest, Int. J. Mass. Spectrom., 239, 87–101, 2004.

Atkinson, R., Baulch, D. L., Cox, R. A., Crowley, J. N., Hampson, R. F., Hynes, R. G., Jenkin, M. E., Rossi, M. J., Troe, J., and IUPAC Subcommittee: Evaluated kinetic and photochemical data for atmospheric chemistry: Volume II – gas phase reactions of organic species, Atmos. Chem. Phys., 6, 3625–4055, doi:10.5194/acp-6-3625-2006, 2006.

Benkelberg, H. J., Boge, O., Seuwen, R., and Warneck, P.: Product distributions from the OH radical-induced oxidation of but-1-ene, methyl-substituted but-1-enes and isoprene in NO_x-free air, Phys. Chem. Chem. Phys., 2, 4029–4039, 2000.

Blake, R. S., Wyche, K. P., Ellis, A. M., and Monks, P. S.: Chemical ionization reaction time-of-flight mass spectrometry: multi-reagent analysis for determination of trace gas composition, Int. J. Mass. Spectrom., 254, 85–93, doi:10.1016/j.ijms.2006.05.021, 2006.

Blake, R. S., Monks, P. S., and Ellis, A. M.: Proton-transfer reaction mass spectrometry, Chem. Rev., 109, 861–896, doi:10.1021/Cr800364q, 2009.

Butler, T. M., Taraborrelli, D., Brühl, C., Fischer, H., Harder, H., Martinez, M., Williams, J., Lawrence, M. G., and Lelieveld, J.: Improved simulation of isoprene oxidation chemistry with the ECHAM5/MESSy chemistry-climate model: lessons from the GABRIEL airborne field campaign, Atmos. Chem. Phys., 8, 4529–4546, doi:10.5194/acp-8-4529-2008, 2008.

Carter, W. P. L., Cocker III, D. R., Fitz, D. R., Malkina, I. L., Bumiller, K., Sauer, C. G., Pisano, J. T., Bufalino, C., and Song, C.: A new environmental chamber for evaluation of gas-phase chemical mechanisms and secondary aerosol formation, Atmos. Environ., 39, 7768–7788, 2005.

Chen, Q., Liu, Y. J., Donahue, N. M., Shilling, J. E., and Martin, S. T.: Particle-phase chemistry of secondary organic material: modeled compared to measured O : C and H : C elemental ratios provide constraints, Environ. Sci. Technol., 45, 4763–4770, doi:10.1021/Es104398s, 2011.

Crounse, J. D., Paulot, F., Kjaergaard, H. G., and Wennberg, P. O.: Peroxy radical isomerization in the oxidation of isoprene, Phys. Chem. Chem. Phys., 13, 13607–13613, doi:10.1039/c1cp21330j, 2011.

da Silva, G., Graham, C., and Wang, Z. F.: Unimolecular beta-hydroxyperoxy radical decomposition with OH recycling in the photochemical oxidation of isoprene, Environ. Sci. Technol., 44, 250–256, doi:10.1021/es900924d, 2010.

de Gouw, J. and Warneke, C.: Measurements of volatile organic compounds in the earths atmosphere using proton-transfer-reaction mass spectrometry, Mass. Spectrom. Rev., 26, 223–257, doi:10.1002/Mas.20119, 2007.

Dillon, T. J. and Crowley, J. N.: Direct detection of OH formation in the reactions of HO_2 with $CH_3C(O)O_2$ and other substituted peroxy radicals, Atmos. Chem. Phys., 8, 4877–4889, doi:10.5194/acp-8-4877-2008, 2008.

Graus, M., Muller, M., and Hansel, A.: High resolution PTR-TOF: quantification and formula confirmation of VOC in real time, J. Am. Soc. Mass. Spectr., 21, 1037–1044, doi:10.1016/j.jasms.2010.02.006, 2010.

Grosjean, D., Williams, E. L., and Grosjean, E.: Atmospheric chemistry of isoprene and of its carbonyl products, Environ. Sci. Technol., 27, 830–840, doi:10.1021/es00042a004, 1993.

Hasson, A. S., Tyndall, G. S., and Orlando, J. J.: A product yield study of the reaction of HO_2 radicals with ethyl peroxy ($C_2H_5O_2$), acetyl peroxy ($CH_3C(O)O_2$), and acetonyl peroxy ($CH_3C(O)CH_2O_2$) radicals, J. Phys. Chem. A, 108, 5979–5989, doi:10.1021/jp048873t, 2004.

Hasson, A. S., Kuwata, K. T., Arroyo, M. C., and Petersen, E. B.: Theoretical studies of the reaction of hydroperoxy radicals (HO_2) with ethyl peroxy ($CH_3CH_2O_2$), acetyl peroxy ($CH_3C(O)O_2$), and acetonyl peroxy ($CH_3C(O)CH_2O_2$) radicals, J. Photoch. Photobio. A, 176, 218–230, doi:10.1016/j.jphotochem.2005.08.012, 2005.

Jenkin, M. E., Saunders, S. M., and Pilling, M. J.: The tropospheric degradation of volatile organic compounds: a protocol for mechanism development, Atmos. Environ., 31, 81–104, 1997.

Jenkin, M. E., Boyd, A. A., and Lesclaux, R.: Peroxy radical kinetics resulting from the OH-initiated oxidation of 1,3-butadiene, 2,3-dimethyl-1,3-butadiene and isoprene, J. Atmos. Chem., 29, 267–298, doi:10.1023/a:1005940332441, 1998.

Jenkin, M. E., Hurley, M. D., and Wallington, T. J.: Investigation of the radical product channel of the $CH_3C(O)O_2 + HO_2$ reaction in the gas phase, Phys. Chem. Chem. Phys., 9, 3149–3162, 2007.

Jenkin, M. E., Hurley, M. D., and Wallington, T. J.: Investigation of the radical product channel of the $CH_3C(O)CH_2O_2 + HO_2$ reaction in the gas phase, Phys. Chem. Chem. Phys., 10, 4274–4280, 2008.

Jordan, A., Haidacher, S., Hanel, G., Hartungen, E., Herbig, J., Märk, L., Schottkowsky, R., Seehauser, H., Sulzer, P., and Märk, T. D.: An online ultra-high sensitivity proton-transfer-reaction mass-spectrometer combined with switchable reagent ion capability (PTR + SRI – MS), Int. J. Mass. Spectrom., 286, 32–38, doi:10.1016/j.ijms.2009.06.006, 2009a.

Jordan, A., Haidacher, S., Hanel, G., Hartungen, E., Märk, L., Seehauser, H., Schottkowsky, R., Sulzer, P., and Märk, T. D.: A high resolution and high sensitivity proton-transfer-reaction time-of-flight mass spectrometer (PTR-TOF-MS), Int. J. Mass. Spectrom., 286, 122–128, doi:10.1016/j.ijms.2009.07.005, 2009b.

Karl, M., Dorn, H. P., Holland, F., Koppmann, R., Poppe, D., Rupp, L., Schaub, A., and Wahner, A.: Product study of the reaction of OH radicals with isoprene in the atmosphere simulation chamber SAPHIR, J. Atmos. Chem., 55, 167–187, doi:10.1007/s10874-006-9034-x, 2006.

Karl, T., Hansel, A., Cappellin, L., Kaser, L., Herdlinger, I., and Jud, W.: Selective measurements of isoprene and 2-methyl-3-buten-2-ol based on NO^+ ionization mass spectrometry, Atmos. Chem. Phys. Discuss., 12, 19349–19370, doi:10.5194/acpd-12-19349-2012, 2012.

King, S. M., Rosenoern, T., Shilling, J. E., Chen, Q., Wang, Z., Biskos, G., McKinney, K. A., Pöschl, U., and Martin, S. T.: Cloud droplet activation of mixed organic-sulfate particles produced by the photooxidation of isoprene, Atmos. Chem. Phys., 10, 3953–3964, doi:10.5194/acp-10-3953-2010, 2010.

Lee, W., Baasandorj, M., Stevens, P. S., and Hites, R. A.: Monitoring OH-initiated oxidation kinetics of isoprene and its products using online mass spectrometry, Environ. Sci. Technol., 39, 1030–1036, doi:10.1021/es049438f, 2005.

Lelieveld, J., Butler, T. M., Crowley, J. N., Dillon, T. J., Fischer, H., Ganzeveld, L., Harder, H., Lawrence, M. G., Martinez, M., Taraborrelli, D., and Williams, J.: Atmospheric oxidation capacity sustained by a tropical forest, Nature, 452, 737–740, 2008.

Mao, J., Ren, X., Zhang, L., Van Duin, D. M., Cohen, R. C., Park, J.-H., Goldstein, A. H., Paulot, F., Beaver, M. R., Crounse, J. D., Wennberg, P. O., DiGangi, J. P., Henry, S. B., Keutsch, F. N., Park, C., Schade, G. W., Wolfe, G. M., Thornton, J. A., and Brune, W. H.: Insights into hydroxyl measurements and atmospheric oxidation in a California forest, Atmos. Chem. Phys., 12, 8009–8020, doi:10.5194/acp-12-8009-2012, 2012.

McKinney, K. A., Lee, B. H., Vasta, A., Pho, T. V., and Munger, J. W.: Emissions of isoprenoids and oxygenated biogenic volatile organic compounds from a New England mixed forest, Atmos. Chem. Phys., 11, 4807–4831, doi:10.5194/acp-11-4807-2011, 2011.

Miyoshi, A., Hatakeyama, S., and Washida, N.: OH radical-initiated photooxidation of isoprene – an estimate of global CO production, J. Geophys. Res., 99, 18779–18787, 1994.

Müller, M., Graus, M., Ruuskanen, T. M., Schnitzhofer, R., Bamberger, I., Kaser, L., Titzmann, T., Hörtnagl, L., Wohlfahrt, G., Karl, T., and Hansel, A.: First eddy covariance flux measurements by PTR-TOF, Atmos. Meas. Tech., 3, 387–395, doi:10.5194/amt-3-387-2010, 2010.

Navarro, M. A., Dusanter, S., Hites, R. A., and Stevens, P. S.: Radical dependence of the yields of methacrolein and methyl vinyl ketone from the OH-Initiated oxidation of isoprene under NO_x-free conditions, Environ. Sci. Technol., 45, 923–929, 10.1021/es103147w, 2011.

Pankow, J. F. and Asher, W. E.: SIMPOL.1: a simple group contribution method for predicting vapor pressures and enthalpies of vaporization of multifunctional organic compounds, Atmos. Chem. Phys., 8, 2773–2796, doi:10.5194/acp-8-2773-2008, 2008.

Paulot, F., Crounse, J. D., Kjaergaard, H. G., Kurten, A., St Clair, J. M., Seinfeld, J. H., and Wennberg, P. O.: Unexpected epoxide formation in the gas-phase photooxidation of isoprene, Science, 325, 730–733, doi:10.1126/science.1172910, 2009.

Paulson, S. E., Flagan, R. C., and Seinfeld, J. H.: Atmospheric photooxidation of isoprene part I: the hydroxyl radical and ground state atomic oxygen reactions, Int. J. Chem. Kinet., 24, 79–101, doi:10.1002/kin.550240109, 1992.

Peeters, J., Nguyen, T. L., and Vereecken, L.: HO_x radical regeneration in the oxidation of isoprene, Phys. Chem. Chem. Phys., 11, 5935–5939, doi:10.1039/B908511d, 2009.

Poisson, N., Kanakidou, M., and Crutzen, P. J.: Impact of non-methane hydrocarbons on tropospheric chemistry and the oxidizing power of the global troposphere: 3-dimensional modelling results, J. Atmos. Chem., 36, 157–230, doi:10.1023/a:1006300616544, 2000.

Rohrer, F., Bohn, B., Brauers, T., Brüning, D., Johnen, F.-J., Wahner, A., and Kleffmann, J.: Characterisation of the photolytic HONO-source in the atmosphere simulation chamber SAPHIR, Atmos. Chem. Phys., 5, 2189–2201, doi:10.5194/acp-5-2189-2005, 2005.

Ruppert, L. and Becker, K. H.: A product study of the OH radical-initiated oxidation of isoprene: formation of C_5-unsaturated diols, Atmos. Environ., 34, 1529–1542, 2000.

Saunders, S. M., Jenkin, M. E., Derwent, R. G., and Pilling, M. J.: Protocol for the development of the Master Chemical Mechanism, MCM v3 (Part A): tropospheric degradation of non-aromatic volatile organic compounds, Atmos. Chem. Phys., 3, 161–180, doi:10.5194/acp-3-161-2003, 2003.

Shilling, J. E., Chen, Q., King, S. M., Rosenoern, T., Kroll, J. H., Worsnop, D. R., DeCarlo, P. F., Aiken, A. C., Sueper, D., Jimenez, J. L., and Martin, S. T.: Loading-dependent elemental composition of α-pinene SOA particles, Atmos. Chem. Phys., 9, 771–782, doi:10.5194/acp-9-771-2009, 2009.

Smith, D. and Spanel, P.: Selected ion flow tube mass spectrometry (SIFT-MS) for on-line trace gas analysis, Mass. Spectrom. Rev., 24, 661–700, doi:10.1002/mas.20033, 2005.

Španěl, P., Ji, Y., and Smith, D.: SIFT studies of the reactions of H_3O^+, NO^+ and O_2^+ with a series of aldehydes and ketones, Int. J. Mass. Spectrom., 165–166, 25–37, 1997.

Španěl, P., Doren, J. M. V., and Smith, D.: A selected ion flow tube study of the reactions of H_3O^+, NO^+, and O_2^+ with saturated and unsaturated aldehydes and subsequent hydration of the product ions, Int. J. Mass. Spectrom., 213, 163–176, 2002.

Sprengnether, M., Demerjian, K. L., Donahue, N. M., and Anderson, J. G.: Product analysis of the OH oxidation of isoprene and 1,3-butadiene in the presence of NO, J. Geophys. Res., 107, 4268, doi:10.1029/2001jd000716, 2002.

Stone, D., Evans, M. J., Edwards, P. M., Commane, R., Ingham, T., Rickard, A. R., Brookes, D. M., Hopkins, J., Leigh, R. J., Lewis, A. C., Monks, P. S., Oram, D., Reeves, C. E., Stewart, D., and Heard, D. E.: Isoprene oxidation mechanisms: measurements and modelling of OH and HO_2 over a South-East Asian tropical rainforest during the OP3 field campaign, Atmos. Chem. Phys., 11, 6749–6771, doi:10.5194/acp-11-6749-2011, 2011.

Tuazon, E. C. and Atkinson, R.: A product study of the gas-phase reaction of isoprene with the OH radical in the presence of NO_x, Int. J. Chem. Kinet., 22, 1221–1236, doi:10.1002/kin.550221202, 1990.

Zhang, Z., Lin, Y.-H., Zhang, H., Surratt, J. D., Ball, L. M., and Gold, A.: Technical Note: Synthesis of isoprene atmospheric oxidation products: isomeric epoxydiols and the rearrangement products cis- and trans-3-methyl-3,4-dihydroxytetrahydrofuran, Atmos. Chem. Phys., 12, 8529–8535, doi:10.5194/acp-12-8529-2012, 2012.

Zhao, J. and Zhang, R.: Proton transfer reaction rate constants between hydronium ion (H_3O^+) and volatile organic compounds, Atmos. Environ., 38, 2177–2185, doi:10.1016/j.atmosenv.2004.01.019, 2004.

Table 1. Summary of experimental conditions and results.

	Chamber Condition[a]	Mixing ratio at steady state (ppb)[d]					Yield (%)[d]	
		NO^+ mode			H_3O^+ mode		MVK	MACR
		Isoprene	MVK	MACR	Isoprene	MVK + MACR		
#1	Main experiment[b]	16.0 ± 0.3	1.3 ± 0.1	0.8 ± 0.1	15.8 ± 0.7	2.1 ± 0.1	4.6 ± 0.3	3.2 ± 0.2
#2	0.5 τ_{ref}	25.4 ± 0.5	1.1 ± 0.1	0.8 ± 0.1	25.2 ± 1.1	2.0 ± 0.1	4.3 ± 0.3	3.4 ± 0.3
#3	2 τ_{ref}	9.5 ± 0.2	1.6 ± 0.1	0.8 ± 0.1	9.3 ± 0.4	2.4 ± 0.1	6.6 ± 0.4	4.3 ± 0.3
#4	0.5 $c[H_2O_2]_{in,ref}$	16.9 ± 0.4	1.7 ± 0.1	1.1 ± 0.1	17.3 ± 0.7	2.7 ± 0.1	6.1 ± 0.3	4.4 ± 0.4
#5	2 $c[H_2O_2]_{in,ref}$	15.8 ± 0.3	1.3 ± 0.1	0.7 ± 0.1	16.2 ± 0.7	2.0 ± 0.1	4.5 ± 0.4	2.8 ± 0.3
#6	2 $c[C_5H_8]_{in,ref}$	34.5 ± 0.7	2.1 ± 0.1	1.6 ± 0.1	34.1 ± 1.5	3.6 ± 0.2	3.7 ± 0.2	3.2 ± 0.2
#7	NO-dominant[c]	18.3 ± 0.4	10.3 ± 0.4	7.9 ± 0.2	18.4 ± 0.8	18.1 ± 0.9	41.1 ± 2.2	28.8 ± 1.2

[a] Experiment #1 is the main experiment. For the other experiments, chamber conditions varied with respect to Experiment #1 are listed. $c[M]_{in,ref}$ represents the inflow mixing ratio of species M for the the main experiment. τ_{ref} is the mean residence time in the chamber for the main experiment. For example, 0.5 $c[H_2O_2]_{in,ref}$ in Experiment #4 indicates that the inflow H_2O_2 mixing ratio for Experiment #4 was half that of the main experiment. Other experimental conditions remain unchanged.

[b] Condition for main experiment: $c[C_5H_8]_{in,ref}$=59 ppb; $c[H_2O_2]_{in,ref}$=16 ppm; no injection of NO_x and measured NO less than minimum detection limit (70 ppt); τ = 3.7 h; 25 °C; < 2 % relative humidity.

[c] Chamber condition for NO-dominant experiment: no injection of H_2O_2; $c[NO]_{in}$ = 28 ppb; other conditions same as those of the main experiment.

[d] (mean value) ± (standard deviation) for mixing ratios and yields. The uncertainties were estimated by Monte Carlo methods (cf. Supplement).

Table 2. Sensitivities of the PTR-TOF-MS to isoprene, MVK, and MACR.

Species	Chemical Formula	NO^+ mode			H_3O^+ mode		
		Product ions	Sensitivity (ncps ppb^{-1})[a]		Product ions	Sensitivity (ncps ppb^{-1})	
			+25 °C[b]	−40 °C[b]		+25 °C	−40 °C
Isoprene	C_5H_8	$C_5H_8^+$	15.7±0.2[c]	15.9±0.3	$C_5H_9^+$	16.8±0.7	16.2±0.6
MVK	C_4H_6O	$C_4H_6O{\cdot}NO^+$	23.1±0.9	23.7±0.6	$C_4H_7O^+$	30.6±1.4	29.2±0.7
MACR	C_4H_6O	$C_4H_5O^+$	15.0±0.4	15.0±0.2	$C_4H_7O^+$	30.0±1.4	28.7±1.1
		$C_4H_6O{\cdot}NO^+$	8.8±0.4	8.9±0.2			

[a] ncps is the measured counts per second (cps) normalized to a primary ion signal of 10^6 cps.
[b] Sensitivities were determined for trap temperatures of +25 and −40 °C.
[c] (mean value) ± (standard deviation) for sensitivities determined across Experiments #1 through #7.

Table 3. Modeled relative importance of competing reaction pathways for Experiments #1 to #7.

	Mixing ratios (ppt)			Reaction rates with ISOPOO (10^{-2} s^{-1})[c]				Contribution by pathway (%)			
	NO[a]	HO_2[b]	$\sum RO_2$[b]	NO	HO_2	RO_2	ISOM	NO	HO_2	RO_2	ISOM
#1	< 70	541	17	1.5	23	0.1	0.2	< 6	93	0.3	0.8
#2	< 70	532	23	1.5	23	0.1	0.2	< 6	93	0.4	0.8
#3	< 70	540	13	1.5	23	0.1	0.2	< 6	93	0.2	0.8
#4	< 70	354	25	1.5	15	0.1	0.2	< 9	89	0.7	1.2
#5	< 70	795	12	1.5	34	0.1	0.2	< 4	95	0.1	0.6
#6	< 70	500	35	1.5	21	0.2	0.2	< 7	92	0.7	0.9
#7	910	28	25	20	1.2	0.1	0.2	93	6	0.5	0.9

[a] Value measured by NO_x analyzer, which had a detection limit of 70 ppt.
[b] Value simulated using MCM v3.2 for the employed reaction conditions.
[c] Reaction rate coefficients of ISOPOO used here: 8.8×10^{-12} cm^3 molec^{-1} s^{-1} for NO, 1.74×10^{-11} cm^3 molec^{-1} s^{-1} for HO_2 (Atkinson et al., 2006), and 0.002 ± 0.001 s^{-1} for isomerization (ISOM, Crounse et al., 2011). A single effective reaction rate coefficient of 1.8×10^{-12} cm^3 molec^{-1} s^{-1} was used for the RO_2 family. This value represents the average reaction rate coefficients of the ISOPOO isomers weighted by their respective branching ratios in MCM v3.2.

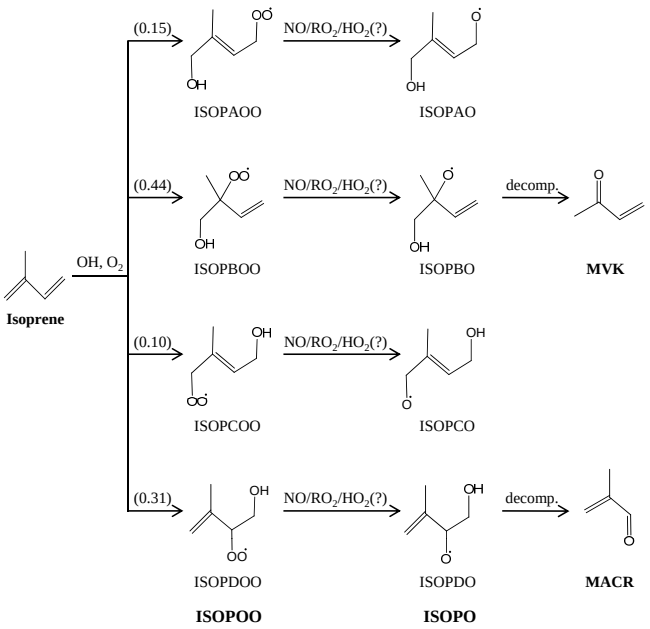

Fig. 1. Mechanism of isoprene oxidation to produce MVK and MACR as first-generation products. Results are shown for NO and RO_2 pathways, as represented in MCM v3.2. Branching ratios to specific products are shown in parentheses. The present study evaluates the extent, represented by the question mark, to which ISOPOO alkyl peroxy radicals might also react with HO_2 to produce ISOPO alkoxy radicals (Reaction R1b) and thereby MVK and MACR (Reactions R2–R3).

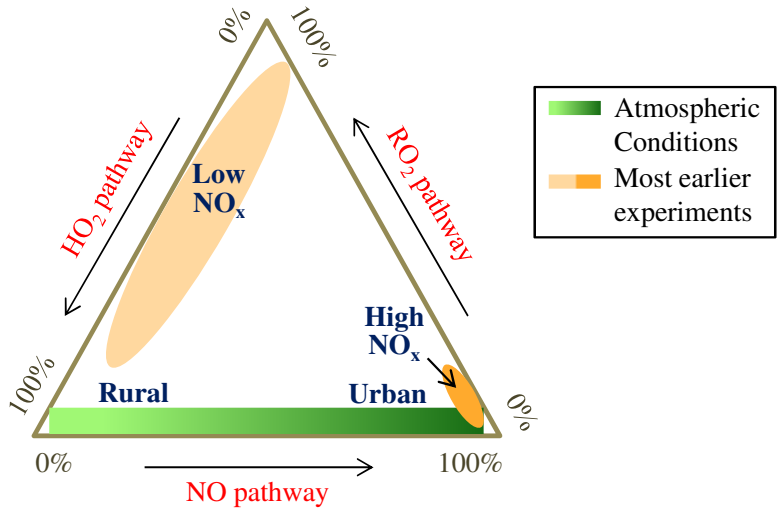

Fig. 2. Diagram of environmental factors that affect the dominant reaction pathways of ISOPOO radicals. The isomerization pathway is not included because of its small contribution in the real atmosphere and in most laboratory experiments.

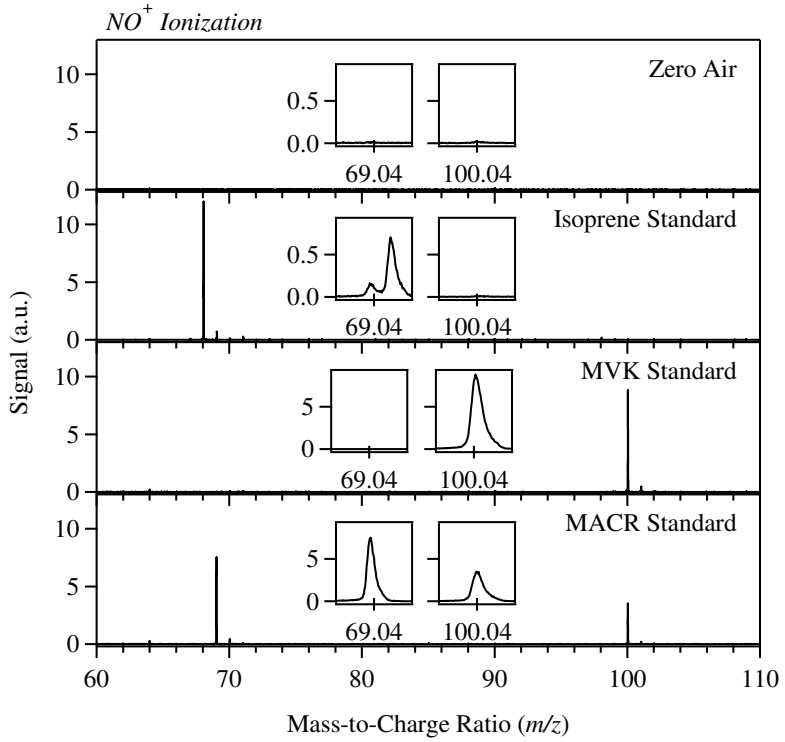

Fig. 3. Mass spectra of zero air, isoprene, MVK, and MACR measured using PTR-TOF-MS with NO^+ reagent ion. Insets show expansions near *m/z* 69 and *m/z* 100, corresponding at *m/z* 69.0335 to $C_4H_5O^+$ contributed by MACR and isoprene, at *m/z* 69.0654 to $C_4^{13}CH_8^+$ contributed by isoprene, and at *m/z* 100.0393 to $C_4H_6O{\cdot}NO^+$ contributed by MVK and MACR.

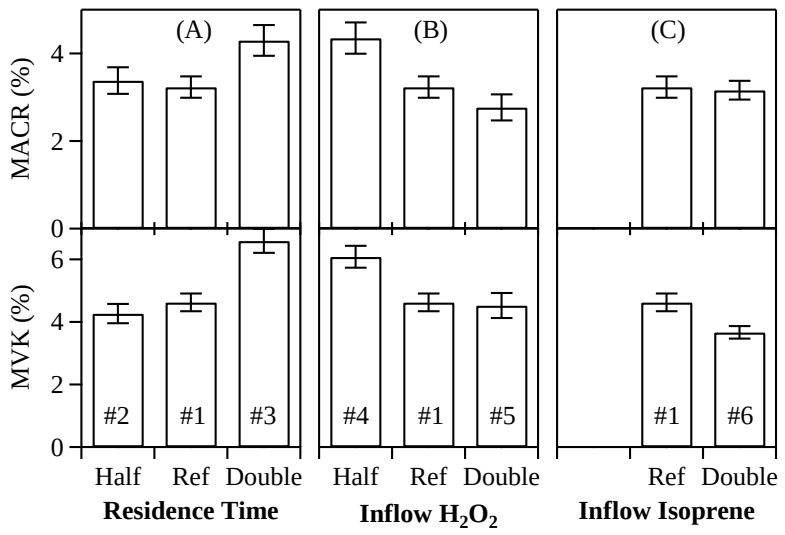

Fig. 4. Measured yields of MACR (top) and MVK (bottom) for HO_2-dominant conditions. **(A)** Variable residence time. **(B)** Variable inflow concentration of H_2O_2. **(C)** Variable inflow concentration of isoprene. The labeled experiment numbers refer to Table 1.

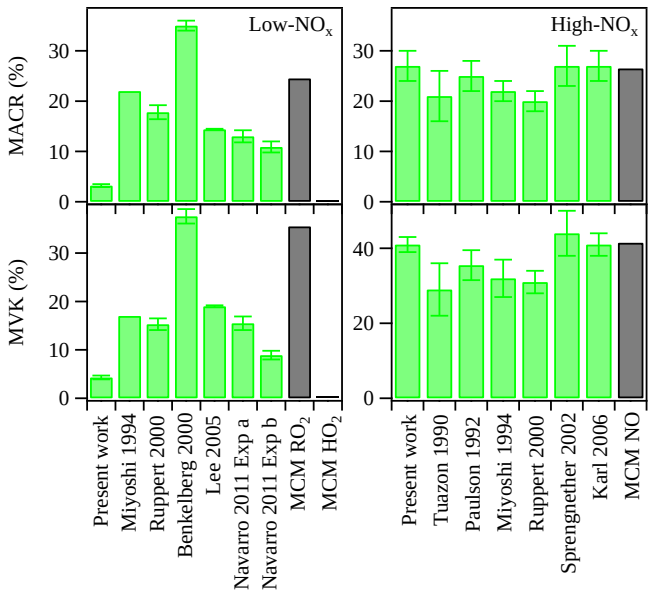

Fig. 5. Comparison of the MVK and MACR yields of this study with those of earlier studies for conditions described as "low NO_x" and "high NO_x" (green bars) and with those of RO_2, HO_2, or NO pathways represented in MCM (grey bars). The "low NO_x" studies might have represented dominant or mixed conditions by RO_2, HO_2, or NO pathways depending on the experimental procedures of each study. Cited studies: Tuazon and Atkinson (1990), Paulson et al. (1992), Miyoshi et al. (1994), Benkelberg et al. (2000), Ruppert and Becker (2000), Sprengnether et al. (2002), Lee et al. (2005), Karl et al. (2006), and Navarro et al. (2011). The modeled ratio of HO_2 to RO_2 is 0.1 and 1 in Navarro 2011 Exp a and Exp b, respectively.

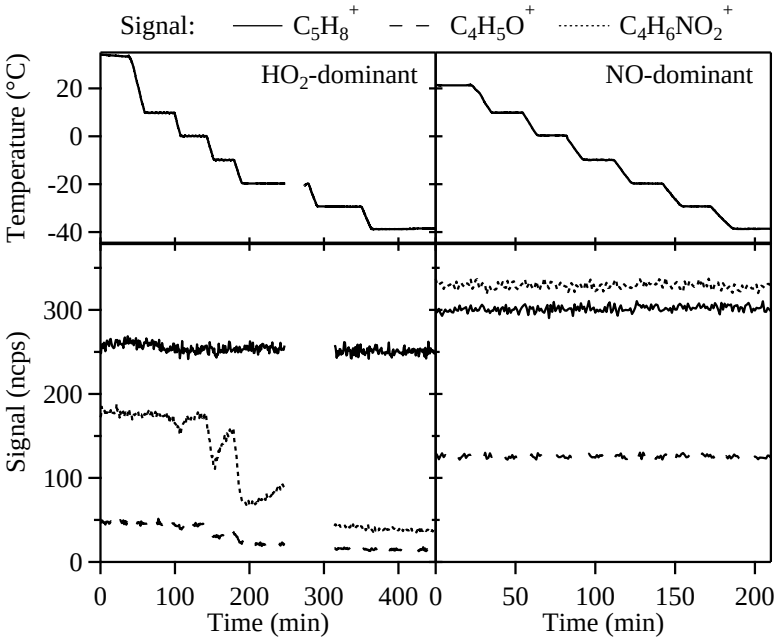

Fig. 6. Time series of (top) trap temperature and (bottom) signal intensities of $C_5H_8^+$ (*m/z* 69.0654), $C_4H_5O^+$ (*m/z* 69.0335), and $C_4H_6NO_2^+$ ions (*m/z* 100.0393). These ions nominally represent isoprene, MACR, and MVK, respectively, when using the NO^+ reagent ion (cf. Fig. S4 for H_3O^+). Results are shown both for HO_2- and NO-dominant conditions (Experiments #1 and #7).